

Efficient Exciton Quenching by Hole Polarons in the Conjugated Polymer MEH-PPV

Ji Yu, Nam Woong Song, Jason D. McNeill, and Paul F. Barbara*

Department of Chemistry and Biochemistry and the Center for Nano- and Molecular Science and Technology,
University of Texas, Austin, Austin, Texas 78712, USA

(Received 1 September 2003 and in revised form 30 October 2003)

Abstract. Recently published near field scanning optical measurements (NSOM) on the conjugated polymer MEH-PPV exhibited a strong dependence of the photoluminescence intensity on the applied electric fields at the NSOM tip. The observed effect is apparently due to exciton quenching by hole polarons. In the present paper, a model “single carrier” electro-modulated-photoluminescence device is used to further explore the exciton quenching effect of hole polarons in MEH-PPV. Hole polarons, created by charge injection from an ITO electrode, are observed to dramatically quench the photoluminescence intensity of MEH-PPV. The Stern–Volmer quenching efficiency of a hole polaron in conjugated polymer thin films was measured to be 390 nm^3 . This value, and other data presented herein, are consistent with the published NSOM photoluminescence modulation measurements and offer further evidence that hole polarons are efficient photoluminescence quenchers in MEH-PPV.

INTRODUCTION

This article is concerned with the quenching mechanism of singlet excitons by hole polarons in conjugated polymers. Charge carriers in conjugated polymers are believed to be highly localized polarons. Polarons in MEH-PPV are localized as a result of both strong vibronic coupling and a high degree of molecular disorder.^{1,2} The mid gap energy states of polarons give rise to nonradiative relaxation pathways for excitons and reduce the photoluminescence (PL) quantum yield of this material.^{3–5} Both polarons and excitons play critical roles in organic opto-electric devices. In an organic light-emitting diode (OLED),^{6,7} for example, charge carriers are injected from electrode to the active media to form electron and hole polarons, which later recombine to generate excitons. Polarons may also be created from dissociation of excitons, which in turn is induced by external electric fields,^{8–12} by a photovoltaic effect,^{13–15} by extrinsic trap states created during processing,^{16,17} or by intentional/unintentional chemical doping.^{18–20} Therefore, a detailed knowledge of the interactions be-

tween polarons and excitons in conjugated polymers is indispensable for the performance optimization of devices based on these materials, such as electro-luminescence displays and solar cells. Additionally, hole-polaron quenching of excitons in poly[2-methoxy, 5-(2'-ethyl-hexyloxy)-*p*-phenylene-vinylene] (MEH-PPV) is apparently also closely related to the poorly understood photooxidation/photo-bleaching mechanism of this material and related conjugated polymers.

Exciton quenching by hole polarons is believed to play an important role in recently described near-field scanning optical microscopy (NSOM) measurements with electrically biased NSOM tips on MEH-PPV.^{3,4} Such experiments offer a promising means for functional imaging of organics devices, such as organic light emitting displays. The NSOM experiments exhibit strong PL intensity modulation (>80%) as a function of electrical bias on the NSOM tip. The electrically biased scanning tip in this type of experiment simultaneously

*Author to whom correspondence should be addressed. E-mail: p.barbara@mail.utexas.edu

optically excites the MEH-PPV and traps polarons in the intense electric field of the biased probe. For a negatively biased tip the PL is strongly quenched, consistent with hole (positive) polaron quenching. In contrast, with a positively biased tip no quenching is observed. In fact, in the presence of oxygen with a positively biased tip the NSOM PL intensity is actually substantially enhanced. The enhancement mechanism is not well established, but apparently involves “repairing” of photooxidation quenching defects by a “reduction” process, since the enhancement is substantially reduced when molecular oxygen levels are reduced by purging the NSOM apparatus with nitrogen. Thus, oxidation/reduction processes are intimately involved in the PL electric field induced modulation mechanism of MEH-PPV.

Unfortunately, quantitative modeling of the NSOM polaron quenching data has not been possible due to the complexity of the polaron generation/recombination dynamics in the tip region and the large uncertainty of the strength and distribution of electric field in the NSOM tip region. This paper presents an alternative, more direct approach to the measurement of exciton quenching by hole polarons. An LED-like device structure is employed in which hole polarons are directly injected from the anode. An insulating layer blocked electron injection from the cathode in order to maintain only one type of polaron in the device (see Fig. 1), i.e., a “single carrier device”.²¹

EXPERIMENTAL

Thin films of MEH-PPV were prepared by spin coating an MEH-PPV/chloroform solution onto an indium tin oxide (ITO)-coated microscope cover glass substrate. The ITO layer serves as the hole injection electrode and has a sheet resistance of 50 ohms. The thickness of the MEH-PPV film (80 nm) is measured by atomic force microscopy (AFM). A 200-nm-thick LiF layer was deposited on top of MEH-PPV, followed by a 200-nm aluminum layer deposited through a mask, making the effective electrode area to be 0.2 cm². Both LiF and Al layers were fabricated by vacuum evaporation. LiF was chosen for its high dielectric constant (~10) and for the ease of thermal evaporation. The LiF layer blocks the electron injection from the Al electrode. Electric pulse train was generated by a function generator and was applied across the ITO and Al electrodes.

RESULTS AND DISCUSSION

Voltage pulse trains of both positive and negative electrical pulses were applied to the blocked-device (see Fig. 1). The recorded PL signal was synchronously averaged over more than 100 cycles of the voltage pulse train. The result shows that PL intensity decreased by

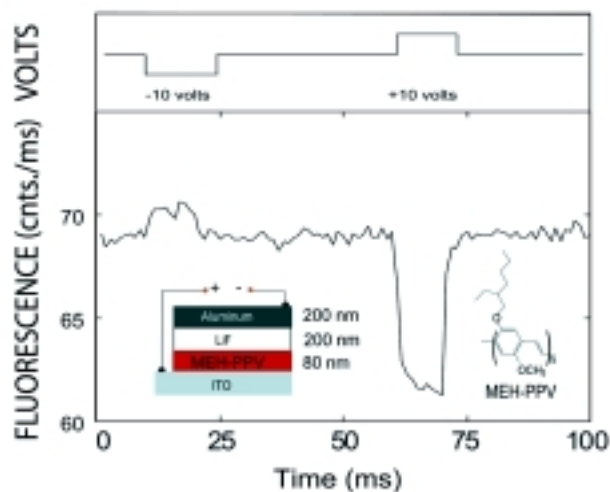


Fig. 1. Electric field photoluminescence device structure and associated data for MEH-PPV. The sign of the bias was defined according to the convention in LED, i.e., positive bias means higher potential on ITO electrode. A 10-Hz frequency was used for all measurements. The duty cycle of the pulse was kept low at 20% to reduce the risk of device breakdown. The leaking current of the blocked device was less than 0.01 μ A. A focused excitation of 488 nm wavelength was applied using a high numerical-aperture (NA) objective (NA = 1.25) on an inverted microscope (Zeiss Axiovert). Excitation area is about 10⁻⁹ cm². The excitation power varies from 0.1 nW to 10 nW. No significant photobleaching of MEH-PPV was observed at this excitation power density.

about 10% under positive bias of 10 V, and increased by 1% under negative bias of -10 V. Both the steady-state PL intensity and the relative changes of the PL amplitude under bias were not sensitive to the choice of the specific area that was illuminated. The transient response of the PL intensity to the “turn-on” of the positive bias has multiple kinetic components. The fast response component that accounts for about 80% of the amplitude change is within the measurement time resolution (1 ms). The slow component is on the millisecond timescale.

The Fermi level in ITO is approximately 0.5 eV above the highest occupied molecular orbital (HOMO) of MEH-PPV. Under the device configuration illustrated in Fig. 1 with a sufficiently positive bias, hole injection should occur at the interface between ITO and the MEH-PPV polymer. Thus, the quenching at positive bias should be assigned to hole polarons quenching. Quenching of the optically produced singlet excitons by hole polarons may involve either an energy transfer mechanism or an electron transfer mechanism, or both,

as described below. The observed PL enhancement effect for negative bias is less well understood than the positive bias quenching effect. Potential assignments for the enhancement effect are given below.

A simple estimate for the steady-state density of hole polarons (n) is available through the capacitance of the LiF layer,

$$n = \frac{(\phi - \phi_{bi})\epsilon}{e} \frac{1}{ld} \quad (1)$$

where ϕ is the electrostatic potential drop across the device, ϕ_{bi} is the built-in potential, ϵ is the permittivity of LiF, e is the electron charge, d is the thickness of the MEH-PPV layer and l is the thickness of LiF layer.

Using the n values from eq 1, the PL data can be analyzed using the Stern-Volmer relation (eq 2) to obtain an estimate for polaron quenching efficiency, K .

$$\frac{I_0}{I} - 1 = Kn \quad (2)$$

Here I_0 is the fluorescent intensity in the absence of hole polarons, I is the measured fluorescent intensity in the presence of hole polarons, and K is quenching efficiency in units of volume per quencher. A plot of the relative quenching amplitude versus bias (Fig. 2) shows the quenching increases linearly with voltage bias. The value of K of 390 nm^3 for hole polarons in MEH-PPV film was derived from the slope of the plot.

It is interesting to compare the experimental result to an estimate based on a diffusion-controlled rate constant (K_{dc}) dynamic quenching model, see eq 2. Since the diffusion constant of polarons is much slower than excitons, we only consider the diffusion of excitons.

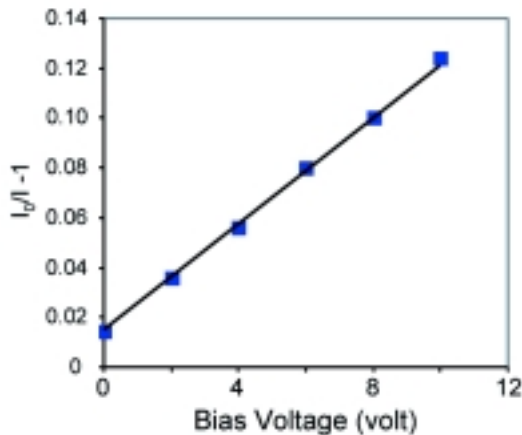


Fig. 2. A Stern-Volmer plot for the steady-state photoluminescence intensity versus bias for an MEH-PPV thin film in the device architecture shown in Fig. 1.

$$K_{dc} = 4\pi r D \tau = 4\pi r l_0^2 \quad (3)$$

Here D is the diffusion constant of excitons, τ is the excited-state lifetime of MEH-PPV, r is the radius of an exciton, and l_0 is the diffusion length of exciton. Estimates in the literature are available for the r (0.6 nm^{23}) and l_0 (7 nm^{23}). The predicted K_{dc} value (370 nm^3) is equal to the measured K within experimental error ($\sim 50 \text{ nm}^3$). This is highly consistent with the polaron quenching mechanism. The actual quenching mechanism is probably more complex than a simple diffusion-controlled process, since the quenching of excitons by polarons should not be well described by a single rate constant in principle, due to material heterogeneity and other non-idealities. Furthermore, the polaron concentration distribution in the polymer film is not expected to be uniform. It should be higher near the LIF blocking layer due to the field. The latter effect would tend to lead to an underestimation of the quenching efficiency when using eq 2.

To fully understand the kinetic response of PL intensity to the bias voltage, the inhomogeneous nature of conjugated polymers in both charge transport and charge injection should be taken into account. Davids et al. have proposed a device model²¹ based on coupled Poisson and continuity equations that allows for such effects. The model had been applied successfully for the modeling of current flow in LED devices.²⁴⁻²⁷ We have adopted this approach to model our device.

$$\frac{\partial n}{\partial t} = \frac{\partial}{\partial z} \left(\frac{\mu k t}{e} \frac{\partial n}{\partial z} - n \mu E \right) \quad (4)$$

$$\frac{\partial(\epsilon E)}{\partial z} = n \quad (5)$$

where n is the number density of hole polarons, μ is the hole mobility, E is electric field, and ϵ is the permittivity. The inhomogeneity of mobility was accounted for by using field-dependent mobilities.

$$\mu = \mu_0 \exp\left(\sqrt{\frac{E}{E_0}}\right) \quad (6)$$

We take μ_0 to be $1.7 \times 10^{-6} \text{ cm}^2/\text{V s}$ and E_0 to be $1 \times 10^{-5} \text{ V/cm}$.²¹ The injection from ITO electrode was assumed to be dominated by thermionic emission,

$$j = AT^2 \left[\frac{n_a}{n_0} - \exp\left(-\frac{\Delta_b}{kT}\right) \right] \quad (7)$$

$$\Delta_b = \Delta_h - e \sqrt{\frac{e|E_a|}{\epsilon_r}} \quad (8)$$

where A is the Richardson constant, n_a is polaron density at anode, n_0 is density of exciton states, Δ_n is interface zero-field Schottky barrier, and ϵ_r is the dielectric constant of polymer. The tunneling injection is not taken into consideration since the injection barrier is high (0.5 eV).²¹ The photon-assisted injection could also be safely ignored here because (1) the excitation power density is low, and (2) any photon-assisted injected polaron will quickly diffuse out of the excitation region and therefore won't accumulate because of the focused excitation.

The result of the calculation is plotted in Fig. 3 along with the experiment data as comparison. The multiple timescale in the response can be understood by considering the strong field-dependent mobility of polarons in conjugated polymers. At early time, there are few charge carriers in the polymer region, and the charging rate is limited by injection at the interface. As the charging process approaches equilibrium, the polaron flux drops dramatically along with the electrical field. Therefore, the injection rate decreases and is limited during this period by the drift rate of polarons inside the polymer.

For positive biases, changing the optical excitation power was observed to have little effect on the quenching amplitude at fixed bias voltage (see Fig. 4), further supporting that the charge injection is thermionic and not photo-assisted. Interestingly, the PL intensity under negative bias, on the other hand, shows a noticeable dependence on the excitation power dependence. It is obviously photo-driven and becomes negligible at low

excitation power. The enhancement observed in the negatively biased device is apparently due to neutralization (by electron polarons or other electron donors) of photo-generated hole polarons or other photo-oxidized forms of MEH-PPV. At zero and negative biases, photo-oxidation routes to oxidized MEH-PPV appear to dominate thermionic production of these species. This effect appears to be analogous to the previously reported enhancement effect in the NSOM data, where photooxidation involving molecular oxygen was the dominant source of oxidized MEH-PPV under conditions where thermionic generation and trapping of hole polarons was not favored. For the devices in this paper, molecular oxygen may also play a role. Although the devices have been prepared in vacuum, it is well known that pinholes in the metal layers allow for small amounts of oxygen to enter devices fabricated by this technique.

It should be emphasized that the observed effects reported herein are not due to electric field induced fluorescence quenching by exciton dissociation into charge pairs.⁸⁻¹² While this effect has been observed in both conjugated polymers it occurs at much greater fields than accessed in the experiments described herein.¹²

A set of charge transfer processes that account for the various effects described herein are outlined in Fig. 5. At low excitation intensity the device properties are dominated by simple exciton generation, thermionic injection hole polarons, and quenching of excitons by hole polarons. At large optical excitation rates, the conjugated

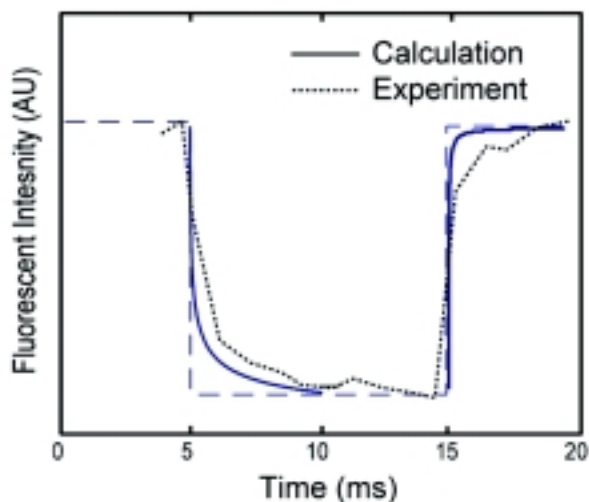


Fig. 3. The dynamics of the fluorescence intensity vs. applied voltage (dashed line) for the device structure shown in Fig. 1. The experimental (dotted line) and theoretical (solid line) curves are in good agreement, supporting the validity of the dynamical model described in the text.

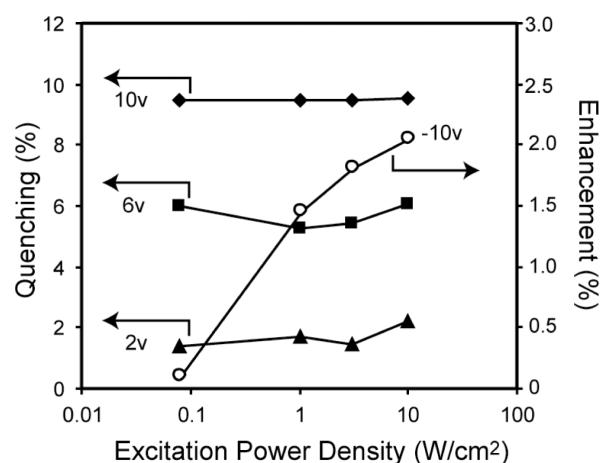


Fig. 4. The MEH-PPV photoluminescence intensity vs. bias voltage and excitation power. The results are represented in terms of percent quenching and percent enhancement, where the zero bias intensity is used as a reference.

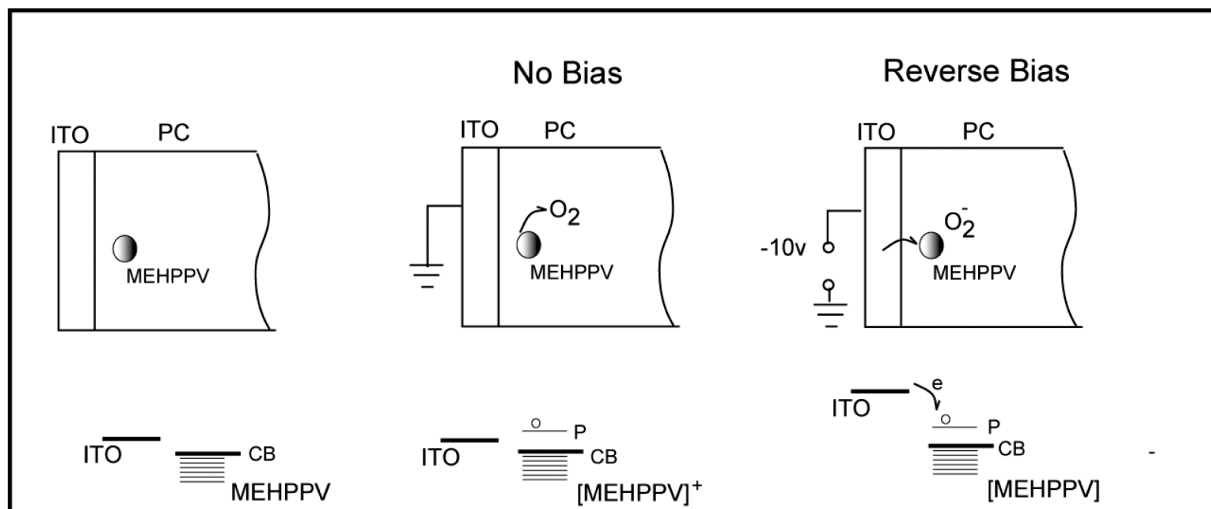


Fig. 5. Energy level diagrams and proposed charge transfer processes that account for the observed effects portrayed in Figs. 1–4.

polymer can undergo photooxidation due, for example, to O_2 impurities. This step leads to the generation of photo-oxidized defects, which can be “repaired” by reduction (electron transfer) in the presence of a negative bias.

CONCLUSION

New measurements on the photoluminescence intensity of MEH-PPV in a single carrier clearly demonstrate that hole polarons are efficient exciton quenchers for the conjugated polymer MEH-PPV. The observed quenching efficiency is estimated to be 390 nm^3 , similar to estimates based on NSOM and other techniques. In addition, it is observed that at high excitation intensities photooxidation in MEH-PPV generates quenching defects that are apparently repairable by reduction when the device is negatively biased.

Acknowledgments. This work was funded by the National Science Foundation and the Robert A. Welch Foundation.

REFERENCES AND NOTES

- (1) Salaneck, W.R.; Stafstrom, S.; Bredas, J.L. *Conjugated Polymer Surfaces and Interfaces: Electronic and Chemical Structure of Interfaces for Polymer Light Emitting Devices*; Cambridge University Press: Cambridge, 1996.
- (2) Antoniadis, H.A.; Abkowitz, M.A.; Hsieh, B.R. *Appl. Phys. Lett.* **1994**, *65*, 2030–2032.
- (3) Adams, D.M.; Kerimo, J.; Liu, C.Y.; Bard, A.J.; Barbara, P.F. *J. Phys. Chem. B* **2000**, *104*, 6728–6736.
- (4) McNeill, J.D.; O’Connor, D.B.; Adams, D.M.; Barbara, P.F.; Kammer, S.B. *J. Phys. Chem. B* **2001**, *105*, 76–82.
- (5) Hieda, H.T.; Tanaka, K.; Naito, K.; Gemma, N. *Thin Solid Films* **1998**, *331*, 152–157.
- (6) Burroughes, J.H.; Bradley, D.D.C.; Brown, A.R.; Marks, R.N.; Mackay, K.; Friend, R.H.; Burn, P.L.; Holmes, A.B. *Nature* **1990**, *347*, 539–541.
- (7) Braun, D.; Heeger, A.J. *Appl. Phys. Lett.* **1991**, *58*, 1982–1984.
- (8) Pfeffer, N.; Neher, D.; Remmers, M.; Poga, C.; Hopmeier, M.; Mahrt, R. *Chem. Phys.* **1998**, *227*, 167–178.
- (9) Deussen, M.; Sshedler, M.; Bassler, H. *Synth. Met.* **1995**, *73*, 123–129.
- (10) Vissenberg, M.; de Jong, M. *Phys. Status Solidi B* **1998**, *205*, 347–350.
- (11) Tasch, S.; Kranzelbinder, G.; Leising, G.; Scherf, U. *Phys. Rev. B: Condens. Matter* **1997**, *55*, 5079–5083.
- (12) Khan, M.I.; Bazan, G.C.; Popovic, Z.D. *Chem. Phys. Lett.* **1998**, *298*, 309–314.
- (13) Yu, G.; Heeger, A.J. *J. Appl. Phys.* **1995**, *78*, 4510–4515.
- (14) Salafsky, J.S. *Phys. Rev. B: Condens. Matter* **1999**, *59*, 10885–10894.
- (15) Marks, R.N.; Halls, J.J.M.; Bradley, D.D.C.; Friend, R.H.; Holmes, A.B. *J. Physics: Condens. Matter* **1994**, *6*, 1379–1394.
- (16) Gomes, H.L.; Stallinga, P.; Rost, H.; Holmes, A.B.; Harrison, M.G.; Friend, R.H. *Appl. Phys. Lett.* **1999**, *74*, 1144–1146.
- (17) List, E.J.W.; Kim, C.H.; Shinar, J.; Pogantsch, A.; Leising, G.; Graupner, W. *Appl. Phys. Lett.* **2000**, *76*, 2083–2085.
- (18) Arias, A.C.; Granstrom, M.; Thomas, D.S.; Petritsch, K.; Friend, R.H. *Phys. Rev. B: Condens. Matter* **1999**, *60*, 1854–1860.
- (19) Huang, F.; Macdiarmid, A.G.; Hsieh, B.R. *Appl. Phys.*

- Lett.* **1997**, *71*, 2415–2417.
- (20) Camaioni, N.; Casalboremiceli, G.; Geri, A.; Nicoletti, S. *Appl. Phys. Lett.* **1998**, *73*, 253–255.
- (21) Davids, P.S.; Campbell, I.H.; Smith, D.L. *J. Appl. Phys.* **1997**, *82*, 6319–6325.
- (22) Gelinck, G.H.P.; Jacob J.; Wegewijs, Bas R.; Mullen, K.; Wildeman, J.; Hadziioannou, G.; Warman, J.M. *Phys. Rev. B: Condens. Matter* **2000**, *62*, 1489–1491.
- (23) Halls, J.J.M.; Pichler, K.; Friend, R.H.; Moratti, S.C.; Holmes, A.B. *Appl. Phys. Lett.* **1996**, *68*, 3120–3122.
- (24) Pinner, D.J.; R.H., F.; Tessler, N. *J. Appl. Phys.* **1999**, *86*, 5116–5130.
- (25) Ruhstaller, B.; Carter, S.A.; Barth, S.; Riel, H.; Riess, W.; Scott, J.C. *J. Appl. Phys.* **2001**, *89*, 4575–4586.
- (26) Hassine, L.; Bouchriha, H.; Roussel, J.; Fave, J.L. *Appl. Phys. Lett.* **2001**, *78*, 1053–1055.
- (27) Lupton, J.M.; Samuel, I.D.W. *Synth. Met.* **2000**, *111*, 381–384.